Chapter 20
Tracking and Removing Modulated Harmonic Components with Spectral Kurtosis and Kalman Filters

Jean-Luc Dion, Cyrille Stephan, Gaël Chevallier, and Hugo Festjens

Abstract This work describes an automatic method for removing modulated sinusoidal components in signals. The method consists in using the Optimized Spectral Kurtosis for initializing Series of Extended Kalman Filters.

The first section is an introduction to vibration applications with Kalman Filters and modulated sinusoids. The detection process with OSK is described in the second section. The third section concerns the tracking algorithm with SEKF for amplitude and frequency modulated sinusoidal components. The last section deals with the complete process illustrated with an experimental application on a rotating machine.

Keywords Kurtosis • Detection • Extended Kaman filter • Frequency modulation • Amplitude modulation • Operational modal analysis

Acronyms

ARMA	Auto Regressive – Moving Average
DOF	Degree Of Freedom
EKF	Extended Kalman Filter
SEKF	Series of Extended Kalman Filters
OMA	Operational Modal Analysis
OSK	Optimized Spectral Kurtosis
PBF	Pass Band Filter
PSD	Power Spectral Density

20.1 Introduction

In the field of Operating Modal Analysis (OMA) applied on structures like helicopters or large structures in energy production, vibration signals are composed with random sources and periodic signals due to rotating machines which can not be shut down. It is a well-known problem that these harmonic components introduce mistakes in experimental modes extraction by OMA algorithms. The present paper intended to solve this problem by tracking and removing modulated sinusoidal signals in noisy records. The previous work has focused on the detection of sinusoidal components [1]. The present work aims to remove these sinusoidal components by using Series of Extended Kalman Filter [2].

J.-L. Dion (✉) • G. Chevallier • H. Festjens
Laboratoire d'Ingénierie des Systèmes Mécaniques et des Matériaux (LISMMA) – EA 2336, SUPMECA Paris 3, rue Fernand Hainaut, 93407 Saint Ouen, France, Tel: 33(0)1 49 45 29 12, Fax: 33(0)1 49 45 29 10
e-mail: jean-luc.dion@supmeca.fr; gael.chevallier@supmeca.fr; hugo.festjens@supmeca.fr

C. Stephan
ONERA, Châtillon, France
e-mail: cyrille.stephan@onera.fr

R. Allemang et al. (eds.), *Topics in Modal Analysis, Volume 7: Proceedings of the 31st IMAC, A Conference on Structural Dynamics, 2013*, Conference Proceedings of the Society for Experimental Mechanics Series 45,
DOI 10.1007/978-1-4614-6585-0_20,

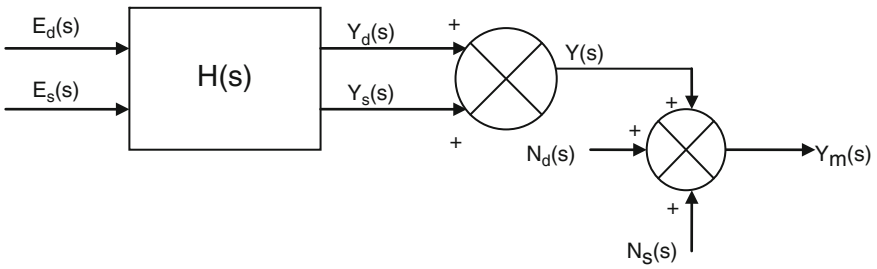

Fig. 20.1 Block diagram of the studied problem. Measured signals $Y_m(s)$ are composed of stochastic and deterministic signals. The aim of the study is to remove the deterministic part in $Y_m(s)$

In the field of vibrations, several works have already used Kalman filters for identification, detection, health monitoring or tracking order. In identification and detection processes, Kalman Filters are performed for the localization of cracks on rotating machines [3], for stiffness identification [4] or vibration force estimation [5,6]. Some health monitoring methods for structures and rotating machines are based on Kalman Filters with varying Auto Regressive identification parameters [7–11]. Kalman Filters are also used in active vibration control [12–15] with real-time algorithms and non-stationary signals on smart structures. Other works use Kalman filters to improve time-frequency analysis and order tracking techniques [16–20]. Order Tracking techniques for rotating machines are often based on Vold-Kalman Filter [21, 22]. Recent techniques aim to improve the Vold Kalman Filtering for resampling techniques, high frequency resolution in Fourier analysis and crossing orders detection [23–30]. Most of these works are based on shaft speed information, as an instantaneous frequency is often measured by tachometers.

The whole process of measurement from an excitation source to measured signals can be depicted in a diagram (see Fig. 20.1). In the rest of this paper, the structure is supposed to have a linear dynamic behavior. Then in a limited bandwidth, the relation between inputs and outputs can be fully captured by its transfer function H(s), defined in the Laplace domain.

This structure is supposed to be excited by two kinds of input. The first one is created by a random source which delivers a white noise. Thus it is a stochastic input named $E_s(s)$. The second one is created by an unbalanced rotating machine. Contrary to the first input, it delivers a signal whose amplitude and frequency are slowly modulated. As the signal slowly changes over time, it has a phase and is deterministic. It is named $E_d(s)$, for deterministic input. Both inputs are not measured.

For a linear structure, the response $Y(s)$ of the structure can be separated into its stochastic and deterministic parts:

$$Y(s) = Y_s(s) + Y_d(s) \tag{20.1}$$

where $Y_s(s) = H(s)E_s(s)$ is the response due to the stochastic input $E_s(s)$ and $Y_d(s) = H(s)E_d(s)$ is the response due to the deterministic input $E_d(s)$.

As errors are unavoidable in measurements, they have to be taken into account too. As for inputs, two kinds of observation noise can distort signals. The first one is a random noise $N_s(s)$ which come from electronic flaws. Its probability law is usually supposed to be Gaussian $p(t) = N(0, W)$ and is characterized in the frequency domain by a flat density of spectral amplitudes, i.e. its energy is uniformly distributed among frequencies.

The second possible noise often results of an electrical field which produces a periodic component at a stable frequency, but with modulated amplitude. Unfortunately this electrical field is also caught by sensors. For instance, in Europe the spurious harmonic components at n^*50 Hz are well known by experimental engineers. This added noise $N_d(f)$ is deterministic and is noticeable in signals as narrow components around its fundamental frequency and its harmonics. From a structural point of view, they look like spurious low-damped modes. Unfortunately, this noise cannot be accurately predicted because it highly depends on each experiment and on each sensor technology. This kind of noise is seldom taken into account, although it can seriously alter signals if structural responses are weak.

In conclusion, the observed signals result in the sum of these noises added to structural responses:

$$Y_m(t) = Y(t) + N_d(t) + N_s(t) \tag{20.2}$$

that can be also separated into its stochastic and deterministic parts:

$$Y_m(t) = Y_s(t) + N_s(t) + Y_d(t) + N_d(t) \tag{20.3}$$

As a rule, OMA are designed for only stochastic input and noise measurement. It is a strong assumption for these algorithms and is seldom respected. As a result, deterministic components in responses can strongly false results given by OMA algorithms.

The purpose of the proposed method is to identify the deterministic part $Y_d(t)$ and to substract it from $Y_m(t)$. It will give an approximation of the stochastic response which would be obtained if E_d and N_d were missing. Then this approximation could be possibly used for OMA identification techniques, although here the focus will be made on the filtering process. Here the term filtering means that the deterministic component of $Y_d(t)$ is going to be filtered from the available signals $Y_m(t)$, without previous knowledge of the structure of $Y_d(t)$.

In the present study, the detection and the tracking of sinusoidal components are performed without the knowledge of frequencies of periodic signal or of a transfer function $H(s)$. Studied signals are assumed to be composed of random noise and modulated sinusoidal components. Indeed, measured signals on rotating engines in operational conditions are:

$$\begin{aligned} &s(t) = b(t) + \sum_k p_k(t) \\ &With \quad b(t) = Y_s(t) + N_s(t) \quad and \quad \sum_k p_k(t) = Y_d(t) + N_d(t) \end{aligned} \tag{20.4}$$

The first term $b(t)$ is assumed to be mainly composed with the structural response under random excitation. The second terms $p_k(t)$ come from engines in operation and from spurious harmonic components of the electric power supply. The signals $p_k(t)$ are deterministic and assumed to be both amplitude and frequency modulated. The kth pseudo periodic source is assumed to be composed of N modulated sines:

$$p_k(t) = \sum_{i=1}^{N} a_{i,k}(t)\cos\left(2\pi i\left(f_{0,k}t + \Delta f_k \int_0^t m_k(\theta)d\theta\right) + \varphi_{i,k}\right) \tag{20.5}$$

where:

$a_{i,k}(t)$ the amplitude for the kth source and the ith sinusoid
$f_{0,k}$ the central fundamental frequency of the kth source
Δf_k the frequency deviation of the kth source
m_k the reduced frequency modulation of the kth source with $MAX\{|m_k|\} \leq 1$
$\varphi_{\mathrm{i,k}}$ the phase of the kth source and the ith sinusoid

In the proposed technique, the frequency modulation is assumed to occur slowly in a short range of variation.

$$\frac{d}{dt}\left(\Delta f_k \int_0^t m_k(\theta)d\theta\right) << f_{0,k} \text{ With } |m_k(t)| < 1 \text{ and } \Delta f_k \ll f_{0,k} \tag{20.6}$$

Two signals are sketched in the time domain in Fig. 20.2: signal A is a frequency and amplitude modulated sinusoid (Fig. 20.2 upper left) and signal B is a narrow bandwidth random noise (Fig. 20.2 lower left). Both signals share the same spectrum magnitude (Fig. 20.2 right), although they have different phase spectras. Thus, for a given PSD or spectrum magnitude where phase information is lost, the original temporal signal can not be identified: it could be either a modulated sinusoid (deterministic) or a random noise (stochastic).

As a result, in the case of structural behavior identification, dynamic responses based on "output only" techniques have to be free of such modulated sinusoidal signals. Thus, the purpose is to remove sinusoidal components, such as unbalanced rotating machines speed or electrical current components, from the original signal. The method is built upon two main steps.

First, all sinusoidal components are detected with an Optimized Spectral Kurtosis (OSK) [1]. Thus, the number of sinusoidal components is identified by the OSK. This process is described in Sect. 20.2.

Secondly, an EKF is built per detected central frequency. Then a set of EKFs is obtained and called a Series of Extended Kalman Filters (SEKF). Its size is defined by the number of identified frequencies. State variables and variances in the EKF are firstly identified with OSK data in order to initialize the SEKF process. This step is developed in Sect. 20.4.1.

Finally, each detected periodic signal is tracked and suppressed from the original signal with the help of a SEKF. These steps are developed in Sect. 20.3 from a theoretical point of view, and numerical applications are exposed in Sect. 20.4.

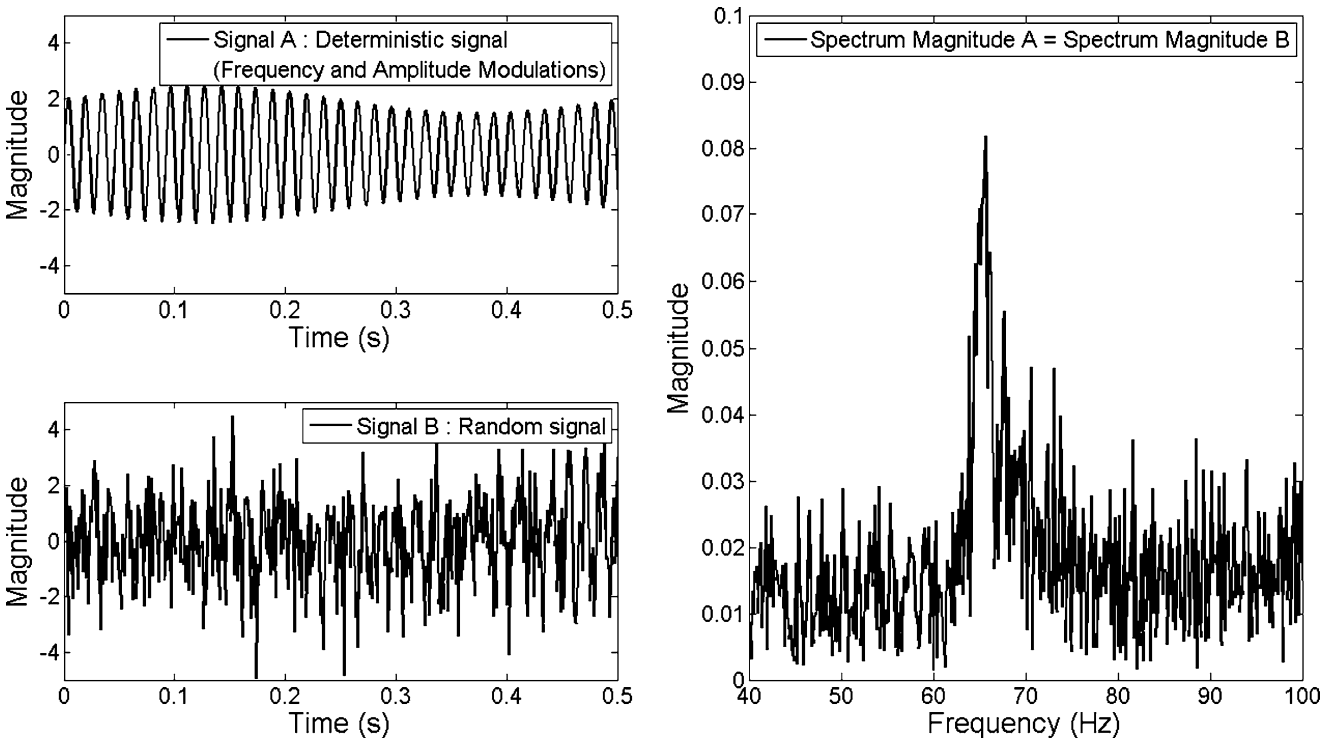

Fig. 20.2 Example of frequency and amplitude modulations of a sinusoid (Signal A: *upper left*), random noise in a narrow bandwidth (Signal B: *lower left*): both signals have the same spectrum magnitude (*right*)

20.2 Detection of Modulated Sinusoidal Components

20.2.1 Definition of the Optimized Spectral Kurtosis Method

The detection of sinusoidal components is based on combining two kinds of information: statistical and spectral as developed in a previous work [1]. The OSK consists in establishing a spectral description of Kurtosis.

First, the signal is filtered with a narrow Pass Band Filter (PBF) centered on the studied frequency.

Secondly, the Kurtosis of the filtered signal is computed and the numerical result defines the assumed nature of the signal (included in the spectral bandwidth). In the ith Pass Band, the ith Kurtosis is defined by:

$$K_i = E\left[\left(\frac{Xf_i - \mu}{\sigma}\right)^4\right] \tag{20.7}$$

where Xf_i is the ith filtered signal obtained from the ith PBF, $\mu = E[X]$, $\sigma^2 = E\left[(X-\mu)^2\right]$ and $E(X)$ is the statistical expectation of X.

The complete spectral description of Kurtosis is obtained by translating the PBF along the entire frequency bandwidth. In order to obtain an accurate spectral resolution, the used PBF is a sixth order Cauer Filter [31] for Real Time Computation but could also be performed with an ideal PBF for Post-Processing Computation. In the case of a real time computation, statistical expectations are computed with the following linear recursive technique:

$$E_k[Y] = \left(1 - \frac{1}{k}\right) E_{k-1}[Y] + \frac{1}{k} y_k \tag{20.8}$$

where y_k is the new data (realization of process Y), $E_{k-1}[Y]$ the old expectation of Y and E_k the new expectation of Y.

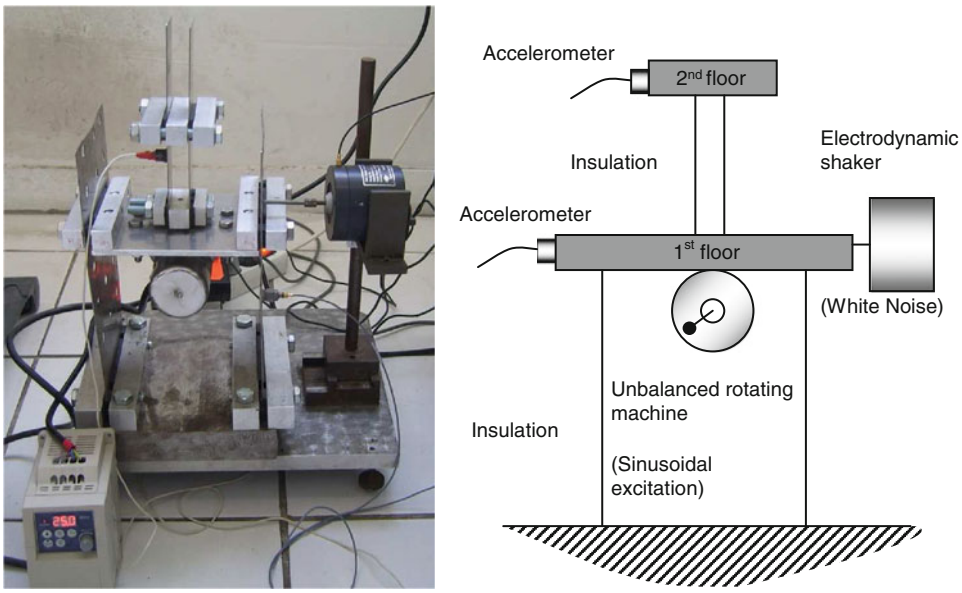

Fig. 20.3 Picture of the bench test. Diagram of the experiment

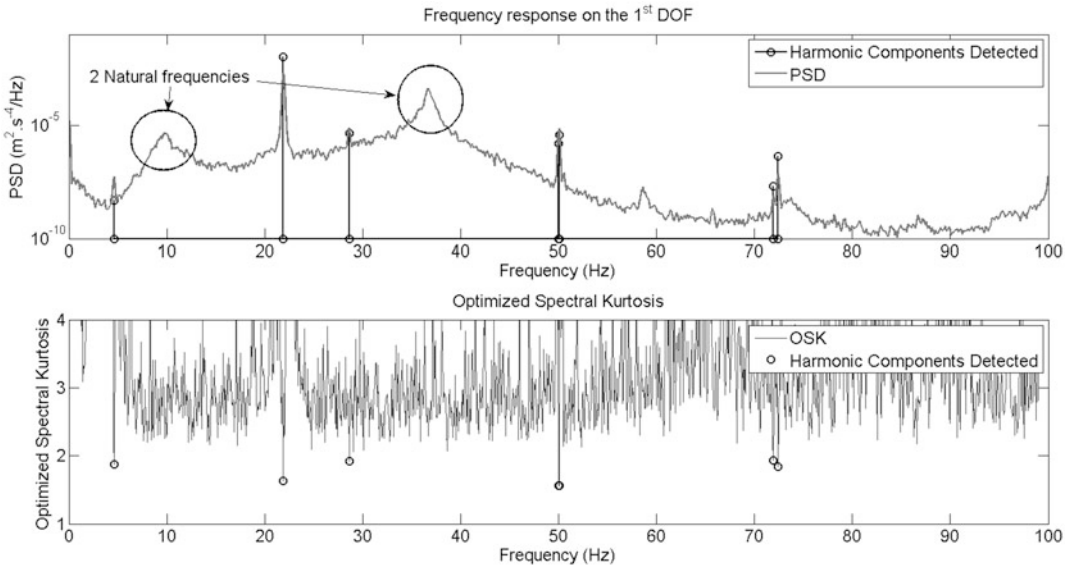

Fig. 20.4 Detection of sinusoidal components using Spectral Kurtosis. One frequency expected but 5 frequencies detected [1]

20.2.2 Testing of the OSK on an Experimental Bench

In order to test the OSK and SEKF in a real experiment, a test bench is set up (Fig. 20.3). The experiment is composed of two masses insulated with flexible blades. The mechanical system can be described as a two DOF system in the bandwidth 0–100 Hz. The system natural frequencies are 9.7 and 36.7 Hz. The structure is simultaneously excited with a white noise by the electrodynamic shaker and an amplitude and frequency modulated signal thanks to an unbalanced rotating machine closed to 1,320 rpm (Fig. 20.3).

Figure 20.4 shows PSD and the OSK applied on a 131 s record of the accelerometer of the first floor with 262,144 (2^{18}) samples. The sampling frequency is 2,000 Hz, the filter bandwidth is around 0.15 Hz, detection is defined for a Spectral Kurtosis lower than two. Detected sinusoidal components are highlighted with "o" markers on both graphs when the OSK is below two [1].

The results shown in Fig. 20.4 highlight expected observations. Frequency $fb = 22$ Hz is well detected as a sinusoidal component and not as a structural response. The corresponding OSK at 22 Hz is lower than two. Duly, both structural eigen

modes (9.7 and 36.7 Hz) are not identified as sinusoidal components. Nevertheless, other components, not initially foreseen, are identified as sinusoidal components: the electric network frequency $fr = 50$ Hz, a low frequency around 5 Hz and two frequencies: $fr - fb = 28$ Hz and $fr + fb = 72$ Hz.

These components are very small but are parts of the signal. The first one is due to the electric power frequency used for the electric motor. The last two are due to the magnitude modulation between the rotation frequency of the engine and its electric power frequency. These components are 100 to 100,000 times smaller than the main excitation at $fb = 22$ Hz.

Measurements have been realized with a piezoelectric accelerometer. Due to this technology, low frequencies are not studied in the present work (even if a 5 Hz component is detected).

The next step consists in removing these components from the original signal.

20.3 Tracking of Modulated Sinusoidal Components

The filtering of modulated sinusoidal components into a composite signal cannot be carried out by classical spectral analysis methods. ARMA filters [31] are not able to separate sinusoidal components and random noise into a same frequency bandwidth. Liftering techniques in cepstral analysis [32] and curve smoothing introduce important distortions in phase spectrum. Instantaneous phases of modulated signals should be accurately determined in order to be tracked. The Extended Kalman Filter has been retained for this purpose.

20.3.1 Discrete State Space Formulation of an Amplitude and Frequency Modulated Sinusoid

The goal of this paragraph is to derive a state space formulation which is relevant on a short time scale.

A sinusoid whose amplitude and frequency are modulated over time can be described in the complex domain as an analytic signal:

$$x(t) = a(t)\ \exp\left(j\phi(t)\right) \tag{20.9}$$

where a(t) is the instantaneous complex amplitude and $\Phi(t)$ is the instantaneous phase. The discrete form of $x(t)$ at the time step $tn = n\Delta t$ is $xn = x(n\Delta t)$. The complex variable x_n can be divided into its real and imaginary parts $x_n = x_{1,n} + jx_{2,n}$. A sinusoid that slightly varies over time can be approximated by:

$$x_n = a_n \exp\left(j\ (2\pi f_n n\Delta t)\right) \tag{20.10}$$

where f_n is the instantaneous frequency.

As the parameters f_n and a_n of the sinusoid slightly vary over time, they are almost equal between two consecutive time steps. Then a transition formulation can be given from x_n to x_{n+1}:

$$x_{n+1} \approx a_n \exp\left(j(2\pi f_n n\Delta t)\right) \times \exp\left(j(2\pi f_n \Delta t)\right) \tag{20.11}$$

This approximation is only true if modulations of a_n and f_n are slower that the period of the sinusoid. This constraint is assumed to be verified. Then a linear transition is obtained between the imaginary part $x_{2,.}$ and real part $x_{1,.}$ of x_n and x_{n+1}:

$$\begin{aligned} x_{1,n+1} &= x_{1,n}.\cos\left(2\pi f_n \Delta t\right) - x_{2,n}.\sin\left(2\pi f_n \Delta t\right) \\ x_{2,n+1} &= x_{1,n}.\sin\left(2\pi f_n \Delta t\right) + x_{2,n}.\cos\left(2\pi f_n \Delta t\right) \end{aligned} \tag{20.12}$$

or written in a matrix form

$$\begin{pmatrix} x_{1,n+1} \\ x_{2,n+1} \end{pmatrix} = \begin{bmatrix} \cos\ (2\pi f_n \Delta t) & -\sin(2\pi f_n \Delta t) \\ \sin\ (2\pi f_n \Delta t) & \cos\left(2\pi f_n \Delta t\right) \end{bmatrix} \begin{pmatrix} x_{1,n} \\ x_{2,n} \end{pmatrix} \tag{20.13}$$

The instantaneous amplitude a_n is given by

$$a_n = \sqrt{x_{1,n}^2 + x_{2,n}^2}. \tag{20.14}$$

As a_n and f_n should be allowed to vary over time, it is proposed here to use the following non linear state space formulation:

$$X_{n+1} = \Phi(X_n) + W_n \tag{20.15}$$

where $X_n = (x_{1,n} x_{2,n} x_{3,n})^T$ and W_n, the process noise. A state variable $x_{3,n} = 2\pi f_n \Delta t$ was added to track the evolution of the instantaneous frequency f_n. The transition between two time steps is composed by a sum of two parts: the stationary part and the evolutionary part.

The stationary part links two successive points of a stationary sinusoid by $\Phi(.)$. Then $\Phi(.)$ is assumed as the non-linear transition function and is given by $\Phi(X_n) = F_n X_n$:

$$\text{where } F_n = \begin{pmatrix} \cos(x_{3,n}) & -\sin(x_{3,n}) & 0 \\ \sin(x_{3,n}) & \cos(x_{3,n}) & 0 \\ 0 & 0 & 1 \end{pmatrix} \tag{20.16}$$

The two first components are related to the complex amplitude and are obtained by the previous linear relation. The third component $x_{3,n+1} = x_{3,n}$ constrains the frequency not to change strongly between two time steps.

Up to now, the non-stationary behavior of the sinusoid was not modeled because it is not possible to express an exact equation for this evolution. We suppose that W_n is a random variable whose probability law is Gaussian: $W_n = N(0, Q)$, where Q is its variance matrix. Then the variations of amplitude and frequency are allowed by random values of W_n.

In a first glance, it could seem strange to choose a random variable for an effect which is generally deterministic. For instance, the variation of frequency excitation of an engine is mainly deterministic. Anyway, this state space does not need to represent accurately the evolution of a sinusoid on a long period, but only step by step. Then on a short time scale, a random evolution of a_n and f_n is enough to model a non-stationary sinusoid.

For a signal composed of M modulated sinusoidal components, the size of the state function is $3M$.

$$F_n(X_n) = \begin{bmatrix} \cos(x_{3,n}) & -\sin(x_{3,n}) & 0 \ldots & 0 & 0 & 0 \\ \sin(x_{3,n}) & \cos(x_{3,n}) & 0 \ldots & 0 & 0 & 0 \\ 0 & 0 & 1 & 0 & 0 & 0 \\ \vdots & \vdots & \ddots & 0 & 0 & 0 \\ 0 & 0 & 0 \ldots \cos\left(x_{3+3(M-1),n}\right) & -\sin\left(x_{3+3(M-1),n}\right) & 0 \\ 0 & 0 & 0 \ldots \sin\left(x_{3+3(M-1),n}\right) & \cos\left(x_{3+3(M-1),n}\right) & 0 \\ 0 & 0 & 0 \ldots & 0 & 0 & 1 \end{bmatrix} \text{ and } X_n = \begin{pmatrix} x_{1,n} \\ x_{2,n} \\ x_{3,n} \\ \vdots \\ x_{1+3(M-1),n} \\ x_{2+3(M-1),n} \\ x_{3+3(M-1),n} \end{pmatrix} \tag{20.17}$$

This state space formulation is non linear: the transition function $\Phi(X_n)$ is varying over time and depends on the frequency modulation.

In reality, only the real part $x_{1,n}$ of the analytic signal x_n can be observed. Unlike the transition phase, the observation phase is completely linear

$$\begin{aligned} Z_n &= [1\ 0\ 0] X_n + V_n \\ Z_n &= \quad x_{1,n} + V_n \end{aligned} \tag{20.18}$$

for one sinusoid and slightly more complex for M sinusoids

$$\begin{aligned} Z_n &= [1\ 0\ 0 \ldots 1\ 0\ 0] X_n + V_n \\ Z_n &= x_{1,n} + \ldots + x_{1+3(M-1)n} + V_n \end{aligned} \tag{20.19}$$

where V_n is a noise observation random process.

Finally, a nonlinear discrete state space model has been derived to model the transition and observation of sinusoid components mixed with random processes

$$\begin{cases} X_{n+1} = \quad \Phi(X_n) + W_n \\ Z_{n+1} = H X_{n+1} + V_{n+1} \end{cases} \tag{20.20}$$

where $\Phi(.)$ is the nonlinear transition function given by $\Phi(X_n) = F(X_n) X_n$ and $H(.)$ is the observation matrix given by:

$$H = [1\ 0\ 0\ \ldots\ 1\ 0\ 0]. \tag{20.21}$$

20.3.2 Application to the Extended Kalman Filter

Kalman filtering refers to a family of algorithms that track the temporal evolution of a dynamic model based on noised measurements:

$$\begin{cases} X_{n+1} = f(X_n, W_n) \\ Z_{n+1} = h\left(X_{n+1}, V_{n+1}\right) \end{cases} \tag{20.22}$$

described here in the discrete time domain. An efficient solution in terms of means and covariances can be derived when $f(.)$ and $h(.)$ are linear. Indeed it estimates the state probability distribution by its two first moments. Unfortunately, they are no longer sufficient to characterize the distribution in the nonlinear case. Then some approximations have to be done in order to find a practical solution.

The extended Kalman filtering is an extension of the classical Kalman filtering to problems with state dynamics governed by nonlinear state transformations. Although it is not required here, it should be noticed that it can also handle a nonlinear transformation from state variables to measurement variables. It generally exhibits a good robustness because it uses linear approximation over small ranges of state space. Without any input control, the state model is defined by the first equation in system (20.22) where W_n is the process noise assumed to be Gaussian with zero mean with a variance matrix Q. The observation model is described by the second equation in system (20.22) where HX_{n+1} is the observation function and V_{n+1} the observation noise assumed to be Gaussian and zero mean with a variance R. State and observation noises are assumed to be uncorrelated. The Extended Kalman Filter [2] is defined using predict and update phases. The predict phase gives an a priori estimate of the state and covariance based on previous time step t_n:

$$\text{Predicted state} \quad \hat{X}_{n+1\,|n} = \hat{F}_{n|n}\hat{X}_{n|n} \tag{20.23}$$

$$\text{Predicted estimated covariance} \quad \hat{P}_{n+1|n} = \tilde{F}_{n|n}\,\hat{P}_{n|n}\,\tilde{F}_{n|n}^{T} + Q \tag{20.24}$$

And the update phase corrects the deviation of these estimations based on new observation at time step t_{n+1}:

$$\text{Innovation } \tilde{Y}_{n+1|n} = Z_{n+1} - H\hat{X}_{n+1|n} \tag{20.25}$$

$$\text{Innovation covariance } S_{n+1} = H\,\hat{P}_{n+1|n}\,H^{T} + R \tag{20.26}$$

$$\text{Kalman gain} \quad K_{n+1} = \hat{P}_{n+1|n}\,H^{T}(S_{n+1})^{-1} \tag{20.27}$$

$$\text{Updated state estimate } \hat{X}_{n+1|n+1} = \hat{X}_{n+1|n} + K_{n+1}\tilde{Y}_{n+1|n} \tag{20.28}$$

$$\text{Updated estimate covariance } \hat{P}_{n+1|n+1} = (I - K_{n+1}H)\hat{P}_{n+1|n} \tag{20.29}$$

As the transition function Φ is non-linear but differentiable, it is well locally approximated thanks to its

$$\text{Jacobian :} \qquad \tilde{F}_{n|n} = \left(\nabla_X \left(F\left(X\right)X\right)^{T}\right)^{T}\Big|_{X=\hat{X}_{n|n}} \tag{20.30}$$

In the case of M modulated components, the first order derivative is required:

$$\nabla X_n = \left(\frac{\partial}{\partial X_{1,n}}\frac{\partial}{\partial X_{2,n}}\cdots\frac{\partial}{\partial X_{3M-1,n}}\frac{\partial}{\partial X_{3M,n}}\right)^{T} \tag{20.31}$$

and the approximation becomes a banded block matrix:

$$\tilde{F}_n = \begin{bmatrix} \tilde{F}_{n,1} & 0 & \dots & 0 \\ 0 & \tilde{F}_{n,2} & \ddots & \vdots \\ \vdots & \ddots & \ddots & 0 \\ 0 & \dots & 0 & \tilde{F}_{n,M} \end{bmatrix} \tag{20.32}$$

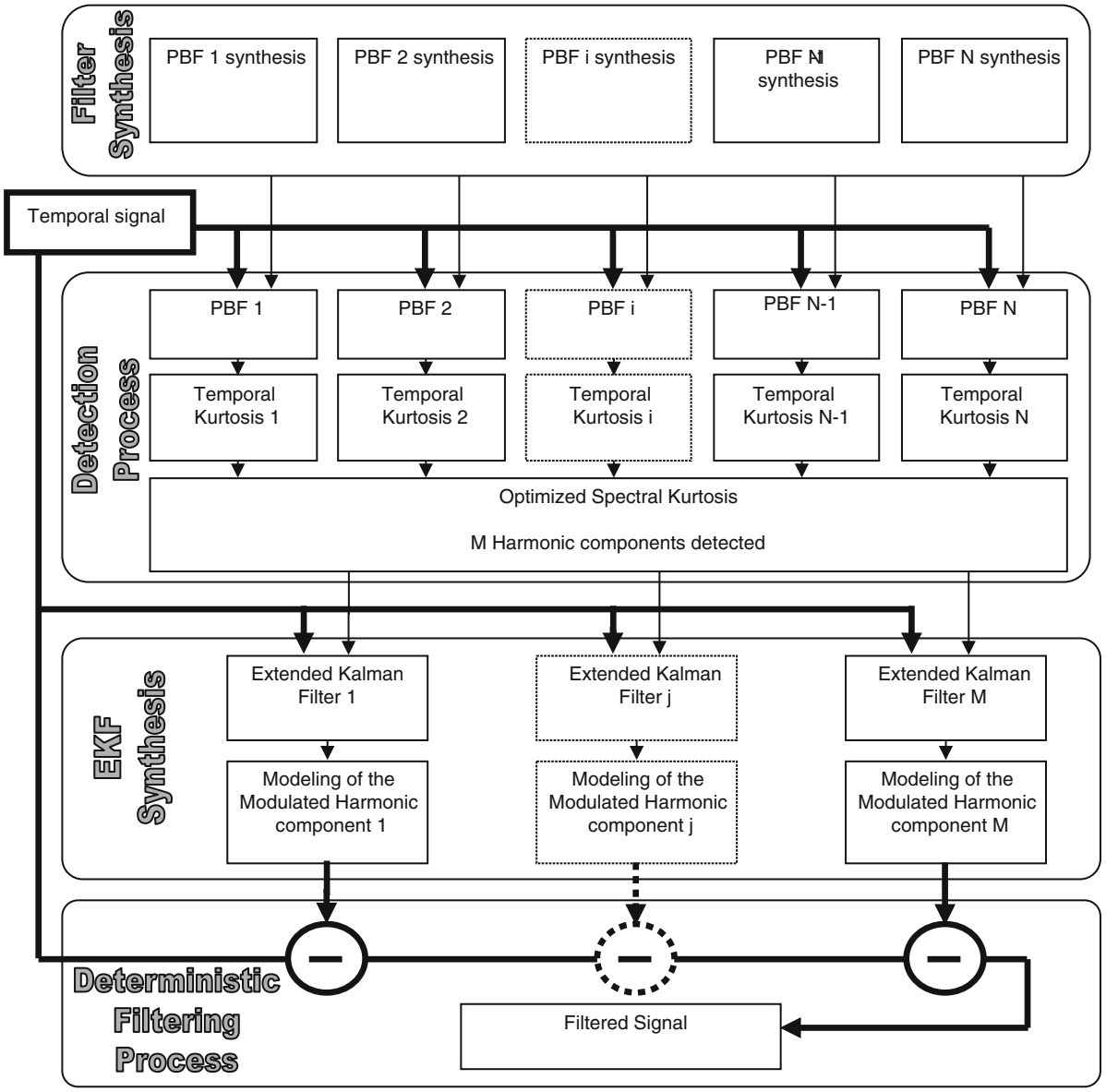

Fig. 20.5 Block diagram of the method. Four main steps in filtering process: filter synthesis (N filters computed off line), sinusoidal components detection with OSK (real time or post-process of M components), Extended Kalman filtering (real time or post-process of M Kalman filters), filtering process (real time or post-process of M modulated sinusoids)

where an elementary block is given by

$$\tilde{F}_{n,i} = \begin{bmatrix} \cos(\hat{x}_{3i,n}) & -\sin(\hat{x}_{3i,n}) & -\hat{x}_{1+3(i-1),n}\sin(\hat{x}_{3i,n}) - \hat{x}_{2+3(i-1),n}\cos(\hat{x}_{3i,n}) \\ \sin(\hat{x}_{3i,n}) & \cos(\hat{x}_{3i,n}) & \hat{x}_{1+3(i-1),n}\cos(\hat{x}_{3i,n}) - \hat{x}_{2+3(i-1),n}\sin(\hat{x}_{3i,n}) \\ 0 & 0 & 1 \end{bmatrix} \tag{20.33}$$

This state matrix is composed of $3M$ equations which could be described as M independent systems of 3 equations. The complete EKF can be expanded in a series of M elementary EKM which could be computed in a same step or in M independent steps. This point of view allows parallel computation of all EKM cells. The complete process is described in the block diagram in next section, Fig. 20.5.

20.4 OSK and SEKF in Operation

In this section, the aim is to propose a method for the filtering process of experimental signals as described in the block diagram (Fig. 20.5).

The filtering process consists in removing detected and tracked sinusoidal components. The efficiency of the method is due to the fact that the OSK allows an accurate initialization of the SEKF. The combination of OSK and SEKF techniques could be performed into two different ways for real time computation or for post-processing computation. These two ways are illustrated in Fig. 20.6.

In order to test the method, the previous Series of EKF have been applied on signals obtained with the test bench described in Sects. 20.2.1 and 20.2.2. Previous results obtained in Sect. 20.2.3 have highlighted 4 modulated components. The tracking of two of them is presented in this section. The first frequency (22 Hz) corresponds to the rotation of the engine and is amplitude and frequency modulated. The second frequency corresponds to the electric power frequency (50 Hz) and is only amplitude modulated.

20.4.1 Initializing the Series of Extended Kalman Filters

An important step for EKF is the estimation of initial parameters conditions. The first unknown parameter is the suitable size of the SEKF. In a second step, for each EKF, several parameters and their variances have to be estimated. The efficiency of the filtering process strongly depends on the quality of estimated initial parameters.

For each EKF, the initial values of nine parameters have to be set:

- Three parameters used for the sinusoidal component modeling,
- Three parameters variances (one per parameter),
- Three process noise variances (one per parameter).

The observation noise variance is defined for the complete SEKF.

For the proposed filtering method based on a SEKF composed of M EKF, $9M+2$ initial conditions have to be estimated. The very first parameter is the number M of EKF. This parameter is defined by the OSK and equal to the number of narrow bandwidths in which detection occurs. The second one is the observation noise variance. The three parameters used to define each sinusoidal component depends on the amplitude, the frequency and the phase of this component.

The estimated amplitude $\tilde{A}_j$ of the jth detected component is determined from the DSP $\overset{\circ}{\gamma}_k$ or the FFT $\overset{\circ}{s}_k$ results:

$$\tilde{A}_j \simeq 2 \underset{k\,|\,f_j=f_k}{\overset{\circ}{s}} \simeq \sqrt{\Delta f \underset{k\,|\,f_j=f_k}{\overset{\circ}{\gamma}}}\,. \tag{20.34}$$

These two estimators overestimate the actual value of A. The higher the frequency is modulated, the larger the overestimation.

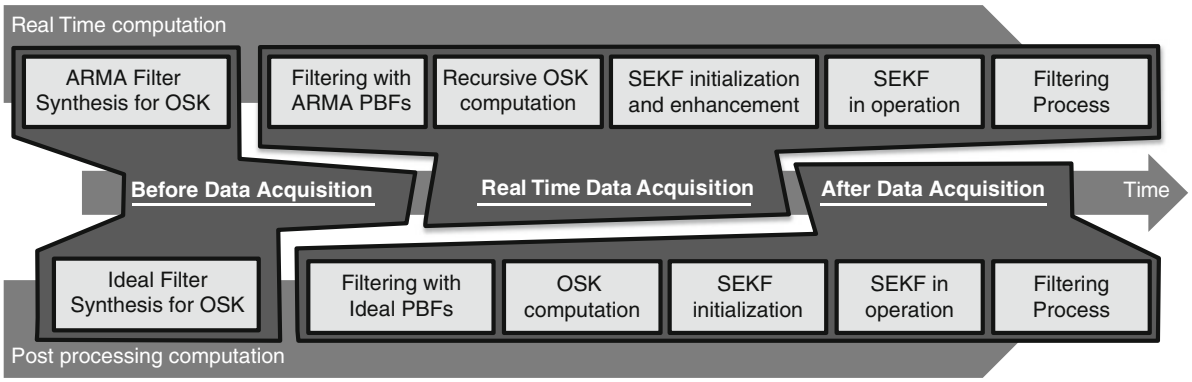

Fig. 20.6 Chronogram of the 2 different ways for combining and computing OSK and SEKF: for real time computation and for post processing computation

The estimated frequency $\tilde{f_j}$ is determined from the OSK and equal to the center frequency f_k of the narrow bandwidth Δf_j in which the detection occurs.

The phase is not estimated and always set in the present method to 0. This lack of estimation is quickly vanished by the specific efficiency of the Kalman Method for this kind of parameter [17].

The jth sinusoidal component modeling is also estimated:

$$\begin{cases} x_{1+3(j-1),0} = \tilde{A}_j \\ x_{2+3(j-1),0} = 0 \\ x_{3+3(j-1),0} = \Delta t 2\pi f_j \end{cases} \tag{20.35}$$

Due to the statistical properties of sinus functions, the estimated variances $\tilde{\sigma}^2_{1+3(j-1)}, \tilde{\sigma}^2_{2+3(j-1)}$ of the first two parameters are:

$$\begin{cases} P_{1+3(j-1),0} = \sigma^2_{1+3(j-1),0} = \frac{1}{2}\tilde{A}^2_j \\ P_{2+3(j-1),0} = \sigma^2_{2+3(j-1),0} = \frac{1}{2}\tilde{A}^2_j \end{cases} \tag{20.36}$$

These estimators underestimate actual variances. The larger the amplitude modulation, the bigger the variance underestimation. For robustness reasons in numerical applications, these parameters are chosen four times bigger.

The estimation of the third variance $\tilde{\sigma}^2_{1+3(j-1)}$ is based on the bandwidth Δf_j in which the detection j occurs:

$$P_{3+3(j-1),0} = \sigma^2_{3+3(j-1),0} = (2\pi \Delta f_j \Delta t)^2 \tag{20.37}$$

The two first process noise variances $Q_{1+3(j-1)}$ and $Q_{2+3(j-1)}$ tend to zero since the modeling of amplitude modulated component is linear. The third process noise variance deals with the frequency modulation and depends on the "velocity" of the frequency modulation. The chosen estimation is:

$$Q_{3+3(j-1)} = \left(\frac{2\pi \Delta f_j \Delta t}{f_j T} \right)^2 \tag{20.38}$$

This approximation can be seen as a linear frequency evolution along Δf_j during the observation time T.

The observation noise variance R is simply chosen equal to the observed signal variance. This approximation is relevant as long as the studied signal is mainly stochastic, i.e. the energy of sinusoid components is weak compared to the total energy of the signal.

20.4.2 Numerical Results and Filtering Efficiency

The SEKF was performed on the previous experiment with two tracked sinusoids previously detected by the OSK. The first component is around 22 Hz and the second around 50 Hz. For each component, the amplitude modulation is determined with the instantaneous amplitude:

$$a_n = \sqrt{x^2_{1,n} + x^2_{2,n}} \tag{20.39}$$

This amplitude could also be obtained by the complex analytic signal composed of the observed signal (real part) and its Hilbert transform (imaginary part).

The frequency modulation is determined by the instantaneous frequency:

$$f_n = \frac{x_{3,n}}{2\pi \Delta t} \tag{20.40}$$

The SEKF provides an analytic signal $\{x_{1,n}, x_{2,n}\}$ per sinusoid from the original signal. Thus one tracked signal is obtained per sinusoid. Spectral amplitudes of these tracked signals show the main components at 22 and 50 Hz and lateral modulated bands (Fig. 20.7).

The first tracked signal concerns the effect of engine rotation. It is characterized by its frequency and amplitude modulations. As it can be observed on the Fig. 20.8, its instantaneous frequency fluctuates between 21.8 and 22 Hz.

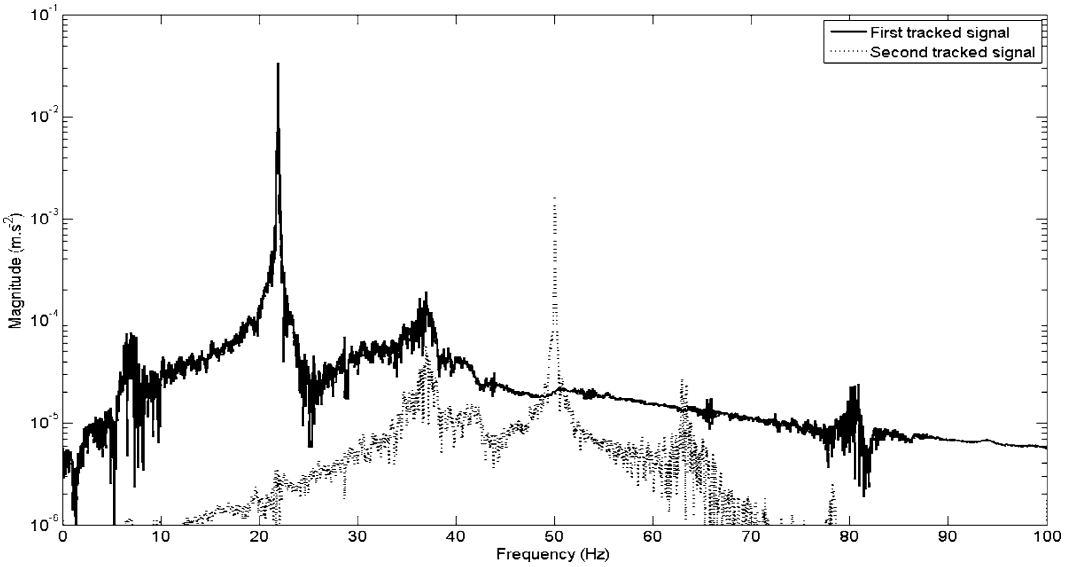

Fig. 20.7 Spectrums of two tracked signals. Symmetric lateral bands are due to modulation effects on spectrums

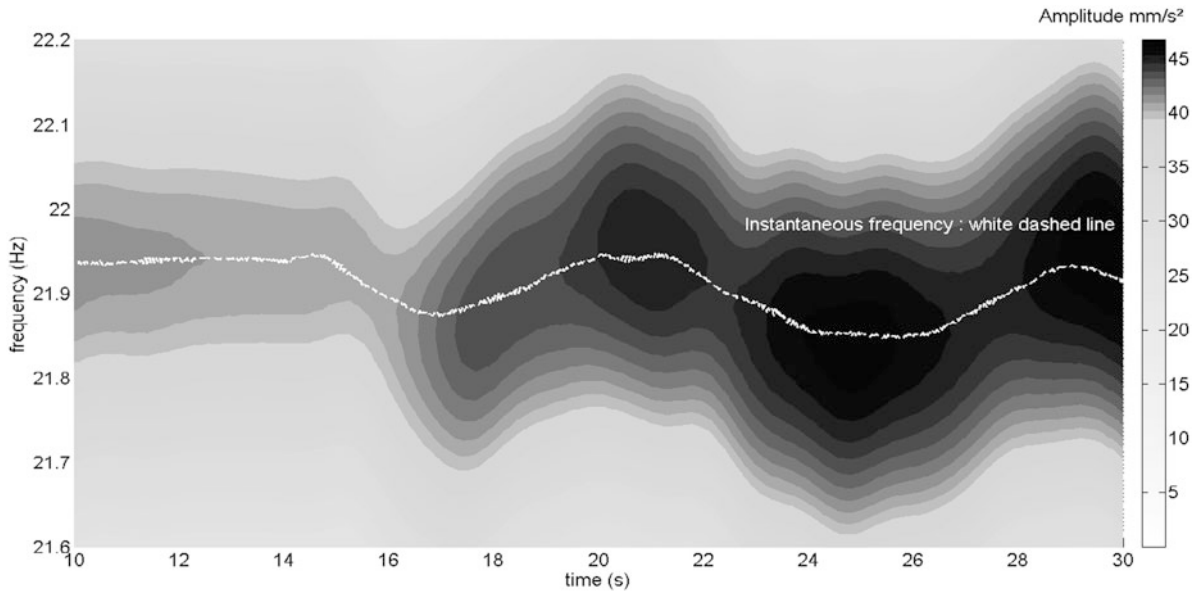

Fig. 20.8 Time-frequency representation of the first tracked signal. Magnitude and frequency modulation are identified with a good accuracy (instantaneous frequency is identified with 4 significant digits)

The second tracked signal is due to the electrical network and is only amplitude-modulated. This property could have been foreseen since the 50 Hz due to the network is absolutely stable in frequency.

The very last step, the effective filtering process, is simply realized in removing the tracked signals from the initial signal in the time domain. Figure 20.9 shows spectral amplitudes before and after the filtering process and for two tracked components (22 and 50 Hz). Although the filtering process removes the 50 Hz component with efficiency, it does not show the same behaviour on the 22 Hz component. This lower efficiency could be explained by the frequency evolution of 22 Hz which makes the tracking harder. However, this component is twenty times lower after the filtering process, which is still a significant improvement.

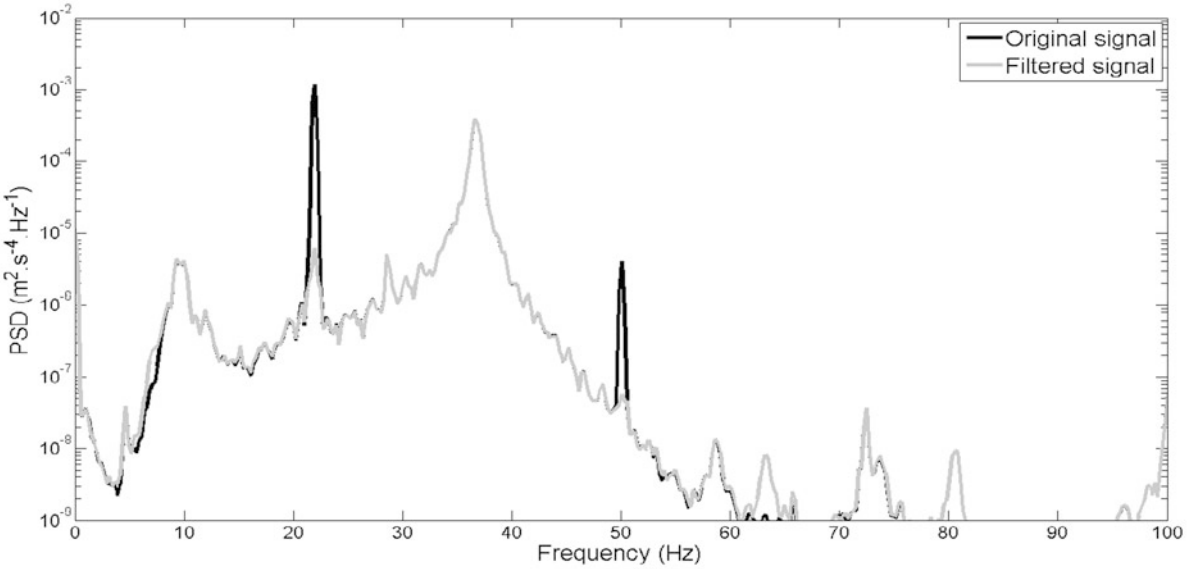

Fig. 20.9 Spectrums before and after the filtering process. The two modulated sinusoidal components are successfully removed

20.5 Conclusion

An important difficulty in the application of Kalman filters is the initialization of state variables and variances. The most important rule of the OSK is to initialize the computation of SEKF. The combination of the Optimized Spectral Kurtosis and Series of Extended Kalman Filters allows a robust computational technique in tracking sinusoidal components. The filtering process can be performed during or after the real time data acquisition. The complete signal filtering can be performed automatically, even if the size of the SEKF is defined by the OSK. Inside the limits of our numerical and experimental tests, the combination of OSK and SEKF allows a robust and efficient way for removing modulated sinusoidal components in signals. The tested method is limited by the frequency modulation rate. Those limits are a new challenge for our work in progress, especially for non smooth non linear systems.

References

1. Dion J-L, Tawfiq I, Chevallier G (2012) Sinusoidal component detection: Optimized Spectral Kurtosis for operational modal analysis. Mech Syst Signal Process 26:24–33
2. Kalman RE (1960) A new approach to linear filtering and prediction problems. Trans Am Soc Mech Eng Ser D – J Basic Eng 82:35–45
3. Seibold S, Weinert K (1996) A time domain method for the localization of cracks in rotors. J Sound Vib 195:57–73
4. Wang Z, Yan W, Shao Y (2009) Three-step method for stiffness identification of inter-story shearing structures under ambient excitation. Tsinghua Sci Technol 14:69–74
5. Ma C-K, Lin D-C, Chang J-M (1999) Estimation of forces generated by a machine mounted upon isolators under operating conditions. J Frankl Inst 336:875–892
6. Ma C-K, Ho C-C (2004) An inverse method for the estimation of input forces acting on non-linear structural systems. J Sound Vib 275:953–971
7. Zhan YM, Jardine AKS (2005) Adaptive autoregressive modeling of non-stationary vibration signals under distinct gear states. Part 1: modeling. J Sound Vib 286:429–450
8. Zhan Y, Mechefske CK (2007) Robust detection of gearbox deterioration using compromised autoregressive modeling and Kolmogorov–Smirnov test statistic. Part I: compromised autoregressive modeling with the aid of hypothesis tests and simulation analysis. Mech Syst Signal Process 21:1953–1982
9. Zhan Y, Mechefske CK (2007) Robust detection of gearbox deterioration using compromised autoregressive modeling and Kolmogorov–Smirnov test statistic. Part II: experiment and application. Mech Syst Signal Process 21:1983–2011
10. Shao Y, Mechefske CK (2009) Gearbox vibration monitoring using extended Kalman filters and hypothesis tests. J Sound Vib 325:629–648
11. Wang G, Luo Z, Qin X, Leng Y, Wang T (2008) Fault identification and classification of rolling element bearing based on time-varying autoregressive spectrum. Mech Syst Signal Process 22:934–947
12. Al-Zaharnah IT (2006) Suppressing vibrations of machining processes in both feed and radial directions using an optimal control strategy: the case of interrupted cutting. J Mater Process Technol 172:305–310

13. Dong X-J, Meng G, Peng J-C (2006) Vibration control of piezoelectric smart structures based on system identification technique: numerical simulation and experimental study. J Sound Vib 297:680–693
14. Marzbanrad J, Ahmadi G, Zohoor H, Hojjat Y (2004) Stochastic optimal preview control of a vehicle suspension. J Sound Vib 275:973–990
15. Yoshimura T, Edokoro K, Ananthanarayana N (1993) An active suspension model For rail/vehicle systems with preview and stochastic optimal control. J Sound Vib 166:507–519
16. Bai M, Huang J, Hong M, Su F (2005) Fault diagnosis of rotating machinery using an intelligent order tracking system. J Sound Vib 280: 699–718
17. Blough JR (2003) Development and analysis of time variant discrete Fourier transform order tracking. Mech Syst Signal Process 17:1185–1199
18. Guo Y, Tan KK (2009) Order-crossing removal in Gabor order tracking by independent component analysis. J Sound Vib 325:471–488
19. Pan M-C, Chiu C-C (2006) Investigation on improved Gabor order tracking technique and its applications. J Sound Vib 295:810–826
20. Pan M-C, Liao S-W, Chiu C-C (2007) Improvement on Gabor order tracking and objective comparison with Vold–Kalman filtering order tracking. Mech Syst Signal Process 21:653–667
21. Vold H, Leuridan J (1993) High resolution order tracking at extreme slew rates, using Kalman tracking filters SAE Paper No. 931288
22. Vold H, Herlufsen H (1997) Multi axle order tracking with the Vold–Kalman tracking filter Sound Vib 31(5):30–34
23. Guo Y, Tan KK (2010) High efficient crossing-order decoupling in Vold–Kalman filtering order tracking based on independent component analysis. Mech Syst Signal Process 24:1756–1766
24. Pan M-C, Lin Y-F (2006a) Further exploration of Vold–Kalman-filtering order tracking with shaft-speed information–I: theoretical part, numerical implementation and parameter investigations. Mech Syst Signal Process 20:1134–1154
25. Pan M-C, Lin Y-F (2006b) Further exploration of Vold–Kalman-filtering order tracking with shaft-speed information–II: engineering applications. Mech Syst Signal Process 20:1410–1428
26. Pan M-C, Wu C-X (2007) Adaptive Vold–Kalman filtering order tracking. Mech Syst Signal Process 21:2957–2969
27. Wang KS, Heyns PS (2011a) An empirical re-sampling method on intrinsic mode function to deal with speed variation in machine fault diagnostics. Appl Soft Comput 11:5015–5027
28. Wang KS, Heyns PS (2011b) The combined use of order tracking techniques for enhanced Fourier analysis of order components. Mech Syst Signal Process 25:803–811
29. Wang KS, Heyns PS (2011c) Application of computed order tracking, Vold–Kalman filtering and EMD in rotating machine vibration. Mech Syst Signal Process 25:416–430
30. Pan M-C, Wu C-X (2010) Extended angular-velocity Vold–Kalman order tracking. J Dyn Syst Meas Control 132(3) doi:10.1115/1.4001326
31. Parks TW, Burrus CS (1987) Digital filter design. Wiley, New York. Chapter 7
32. Randall RB (2001) Cepstrum analysis. In: Ewins D, Rao SS, Braun S (eds) Encyclopedia of vibration. Elsevier, Oxford, pp 216–227